

Effects of dihydroartemisinin combined with cisplatin on proliferation, apoptosis and migration of HepG2 cells

QI RAO*, RUOCHAN LI*, HE YU, LEI XIANG, BIN HE, FENGHUA WU and GANG ZHAO

Department of Medical Biology, School of Basic Medical Sciences,
Hubei University of Chinese Medicine, Wuhan, Hubei 430065, P.R. China

Received November 2, 2021; Accepted May 30, 2022

DOI: 10.3892/ol.2022.13395

Abstract. Cisplatin (DDP) is a potent and widely applied chemotherapeutic agent. However, its clinical efficacy for the treatment of liver cancer is limited by adverse effects and the development of resistance. Combinatorial therapy may alleviate these issues. Dihydroartemisinin (DHA) is a first-generation derivative of artemisinin. The effects of DDP on liver cancer when applied in combination with DHA have not previously been studied. Therefore, the present study aimed to investigate the effects of DHA combined with DDP on HepG2 cells and their potential underlying molecular mechanisms. HepG2 cells were treated with different concentrations of DHA and/or DDP. Cell Counting Kit-8 assay was used to assess the cell viability. Cell proliferation and apoptosis were quantified using flow cytometry, acridine orange/ethidium bromide (AO/EB) fluorescent dual staining and the colony formation assay. Cell migration was quantified using the Transwell and wound healing assays. The HepG2 cell protein expression levels of Fas, Fas-associated death domain (FADD), procaspase-3, cleaved caspase-3, pro-caspase-8, cleaved caspase-8, Bax, Bcl-2, E-cadherin and N-cadherin, were detected via western blotting. Gelatin zymography was used to assess the levels of MMP-9 secreted by HepG2 cells into the supernatant. Following combined DHA and DDP treatment, the percentage of apoptotic cells was significantly increased, whereas cell proliferation and migration were significantly reduced, compared with cells treated with DDP only. DHA and DDP in combination significantly inhibited the expression of MMP-9, significantly increased the protein expression levels of Fas,

FADD, Bax and E-cadherin, significantly increased the ratio of cleaved caspase-3 and cleaved caspase-8 to their precursor proteins and significantly decreased the protein expression levels of Bcl-2 and N-cadherin. The findings of the present study suggested that, DHA may confer synergistic effects with DDP in potentially promoting apoptosis and inhibiting the epithelial-mesenchymal transition for the treatment of liver cancer.

Introduction

Liver cancer is the sixth most commonly diagnosed cancer in the world, with ~906,000 new cases and 830,000 cases of mortality in 2020 (1). Moreover, liver cancer is characterized by late onset, rapid progression and high rates of metastasis (2). As the majority of patients newly diagnosed with liver cancer are already at advanced stages of disease, this disease is associated with a poor prognosis and high fatality rate (3). Comorbidities such as cirrhosis, hydroperitoneum and severe liver dysfunction render advanced liver cancer almost untreatable, even using surgical resection or ablation (4). Epithelial-mesenchymal transition (EMT) is defined as the transformation of epithelial cells into a phenotype with mesenchymal cells, increasing the metastatic capacity and therapeutic resistance of the tumor (5). Furthermore, the application of chemotherapy is limited by the occurrence of adverse side effects and the development of resistance (6). Therefore, novel treatment options are in high demand. Over the past decade, naturally occurring compounds have received widespread attention as potential anti-cancer drugs or sensitization agents (7).

Cisplatin (DDP) is a chemotherapeutic agent that is widely applied in clinical practice and induces cytotoxicity via binding to DNA to induce cell apoptosis (8). The Fas receptor and mitochondrial signaling pathways serve key roles in the apoptotic process of tumor cells following DNA damage induced by DDP (9). DDP is highly effective in the treatment of various tumors, such as testicular, ovarian, bladder, cervical, esophageal, small-cell lung cancers and liver cancer (8). However, it has significant disadvantages, with the most important being cancer cell resistance and numerous harmful side effects (10-12). High DDP doses are one of the main causes of drug resistance and side effects, which frequently result in treatment failure (13). Therefore, enhancing the anti-tumor

Correspondence to: Professor Gang Zhao or Professor Fenghua Wu, Department of Medical Biology, School of Basic Medical Sciences, Hubei University of Chinese Medicine, 16 Huangjiahu West Road, Wuhan, Hubei 430065, P.R. China
E-mail: zgcc66@163.com
E-mail: wfh0101@163.com

*Contributed equally

Key words: dihydroartemisinin, cisplatin, hepatoblastoma cells, proliferation, apoptosis, migration

activity of DDP, whilst decreasing the potency of its adverse effects, has become a key focus of cancer research.

Artemisinin and its derivatives have been widely used for the treatment of malaria since it was discovered and extracted by Tu Yoyo from *Artemisia annua* L., Asteraceae, a herb that has been recorded and used in ancient China for >2,000 years (14). Dihydroartemisinin (DHA) is produced from artemisinin via the reduction of the C-10 carbonyl group, which improves bioavailability and solubility (15,16). In addition to its anti-malarial properties, previous studies have reported the anti-cancer potential of DHA, including against lung cancer, breast cancer and digestive system tumors (17,18). The induction of apoptosis in tumor cells is an important mechanism underlying the anti-tumor effects of DHA. Previous study demonstrated that blocking the induction of cell apoptosis after the formation of the DDP-DNA adducts is responsible for DDP resistance (9). Therefore, it can be hypothesized that DDP combined with DHA may increase the apoptotic rate of tumor cells. Moreover, the ability of tumor cells to proliferate and migrate should be explored following treatment with DDP combined with DHA.

In the present study, HepG2 cells were used as an *in vitro* model of liver cancer to investigate the effects of DHA combined with DDP. It was hypothesized that the efficacy of a lower dose of DDP combined with DHA was equal to or even greater than that of a higher dose of DDP alone. The aim of the present study was to investigate the role of DHA in combination with DDP for the treatment of liver cancer and to provide experimental data for the clinical use of DHA.

Materials and methods

Cell culture and reagents. The liver cancer HepG2 cell line was purchased from The Cell Bank of Type Culture Collection of The Chinese Academy of Sciences. The cells were cultured in RPMI-1640 medium (HyClone; Cytiva), supplemented with 10% FBS (Hangzhou Sijiqing Biological Engineering Materials Co., Ltd.), 100 U/ml penicillin and 100 U/ml streptomycin at 37°C in a humidified incubator supplied with 5% CO₂. The culture medium was replaced every 1-2 days. DHA (Fig. 1A) was purchased from Dalian Meilun Biology Technology Co., Ltd. DDP was purchased from Qilu Pharmaceutical Co., Ltd.

Cell grouping. As previously described (19,20), HepG2 cells were treated at 37°C for 24 h with six treatment groups as follows. i) Control (0 µM DHA and 0 µg/ml DDP); ii) DHA (100 µM DHA); iii) medium-dose (MD) DDP (15 µg/ml DDP); iv) high-dose (HD) DDP (20 µg/ml DDP); v) DHA + low-dose (LD) DDP (100 µM DHA combined with 10 µg/ml DDP); and vi) DHA + MD DDP (100 µM DHA combined with 15 µg/ml DDP).

Cell counting kit-8 (CCK-8) assay. Cells were treated with different concentrations of DHA (37.5, 50, 75, 100, 150, 300 and 400 µM) and DDP (5, 7.5, 10, 15, 20, 30 and 40 µg/ml) for 24 h or aforementioned concentrations of DHA and/or DDP 24-48 h at 37°C and their effects on cell viability was assayed by CCK-8 assay. Specifically, cell suspension (200 µl) containing a total of 4x10³ cells was seeded into each well of a 96-well plate. After 12 h of incubation at 37°C in a humidified

atmosphere containing 5% CO₂, the culture medium in each well was replaced with indicated concentration of DHA or DDP. In total, six duplicate wells were used for each group. The cells were treated for 24 h at 37°C, following which the culture medium was replaced with 200 µl PBS containing 10% CCK-8 (Dalian Meilun Biology Technology Co., Ltd.). Following 2 h of incubation, the viability of HepG2 cells was assessed at an absorbance of 450 nm using a microplate reader. Cell viability was quantified using the following formula: Inhibitory rate (%)=[(1-optical density at 450 nm for the treatment)/optical density at 450 nm for the control] x100.

Colony formation assay. HepG2 cells were seeded into a six-well plate at a density of 500 cells/well for 2 days at 37°C, the aforementioned concentrations of DHA and/or DDP were added to the wells followed by incubation for 12 h at 37°C, before the medium was replaced with fresh RPMI-1640 medium supplemented with 10% FBS, 100 U/ml penicillin and 100 U/ml streptomycin. After 2 weeks of incubation at 37°C with 5% CO₂, the colonies were fixed using anhydrous ethanol (≥99.7%) for 15 min at room temperature and stained with 10% Giemsa (Beyotime Institute of Biotechnology) for 15 min at room temperature, before the number of colonies (>50 cells) in each well was quantified using ImageJ 1.8.0. (National Institutes of Health).

Flow cytometry. The FITC-Annexin V/PI Apoptosis Kit was purchased from Tianjin Sungene Biotech Co., Ltd. 1x10⁶ per well HepG2 cells were treated with the aforementioned concentrations of DHA and/or DDP for 24 h at 37°C. Following treatment, cells were collected using trypsin without EDTA. Cells were resuspended in 400 µl binding buffer followed by incubation with 5 µl FITC-Annexin V for 30 min and 10 µl PI for 30 min at room temperature, which were added in turn, in the dark. The fluorescent cells were then detected using a BD FACSCalibur™ flow cytometer (BD Biosciences) and the results were analyzed using FlowJo X 10.0.7 (FlowJo LLC).

Acridine orange (AO)/ethidium bromide (EB) dual staining assay. AO/EB fluorescence staining was used to detect any morphological changes associated with cell apoptosis. HepG2 cells were seeded onto a round coverslip placed in six-well plates at a density of 5x10⁵ cells per well. After 12 h of incubation at 37°C, the medium in each group was replaced with the aforementioned concentrations of DHA and/or DDP before further incubation for 24 h at 37°C. Cells that attached to the coverslips were stained using AO/EB (AO, cat. no. 158550-10G; EB, cat. no. E8751-5G; Sigma-Aldrich; Merck KGaA) for 5 min at room temperature. Fluorescence microscopy (model 80i; Nikon Corporation) was used to observe the morphology of any apoptotic cells in five randomly selected fields of view. The apoptotic rate was assessed as a percentage from the number of apoptotic cells among 1,000 cells counted per well.

Wound healing assay. A total of 1x10⁶ per well HepG2 cells were seeded in six-well plate. Following incubation for 12 h at 37°C, confluent cell monolayers were scratched using 20-µl pipette tips, before any cells detached were washed away with PBS. Images were then captured of each group at 0 h using an inverted light microscope (model CK-40; Olympus

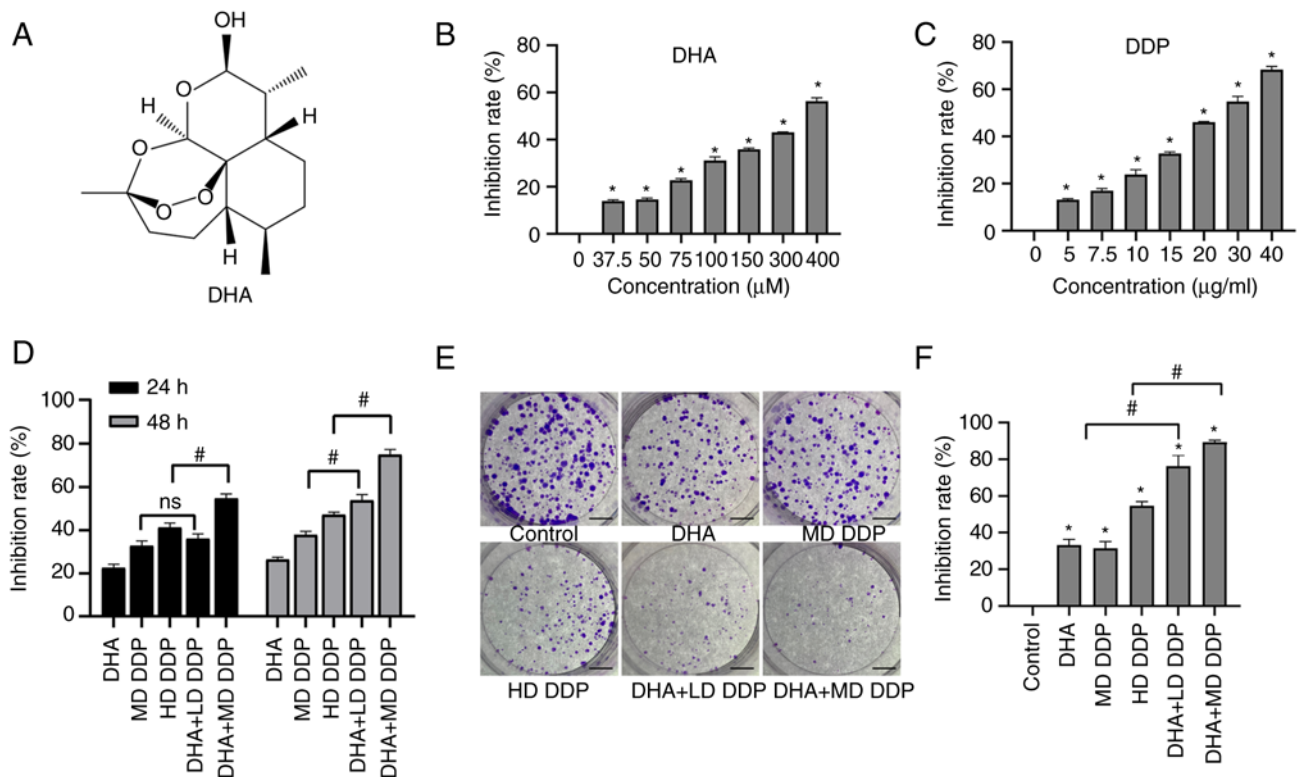


Figure 1. Inhibitory effects of DHA (100 μM) combined with DDP on the viability and proliferation of HepG2 cells. (A) Molecular structure of DHA. (B) Inhibition rate of HepG2 cells treated with different concentrations of DHA for 24 h. (C) Inhibition rate of HepG2 cells treated with different concentrations of DDP for 24 h. (D) Inhibition rate of HepG2 cells treated with DHA and/or DDP for 24 and 48 h. (E) Colony formation of HepG2 cells treated with DHA and/or DDP. Scale bar, 10 mm. (F) Inhibitory rate of DHA and/or DDP on the proliferation of HepG2 cells calculated from the colony formation assay. Data are presented as the mean ± SD of more than three independent experiments. *P<0.05 vs. control; #P<0.05; ns, not significant. DHA, dihydroartemisinin; DDP, cisplatin; LD, low dose (10 μg/ml); MD, medium dose, (15 μg/ml); HD, high dose, (20 μg/ml).

Corporation) before the cells were incubated with serum-free medium at 37°C containing the aforementioned concentrations of DHA and/or DDP for 24 h. Wound healing images were obtained at the same location in the well, which was marked. The migration rate was determined via quantification of the area change of the wound using ImageJ 1.8.0. (National Institutes of Health).

Transwell migration assay. The migratory ability of HepG2 cells was assessed using a Transwell chamber (8 μm; Corning, Inc.). Cells were seeded into the upper chamber at a density of 2x10⁵ cells/well and were suspended in serum-free medium after being treated with the aforementioned concentrations of DHA and/or DDP in a six-well plate for 24 h at 37°C. The bottom chamber contained 600 μl medium containing 10% FBS. After being incubated at 37°C in 5% CO₂ for 24 h, cells that had failed to migrate and remained on the upper membrane surface were wiped away using cotton swabs. Migrated cells were fixed in anhydrous ethanol (≥99.7%) at room temperature for 10 min and stained with 10% Giemsa (Beyotime Institute of Biotechnology) at room temperature for 15 min. Migratory cells were then manually counted in five random fields using an inverted light microscope (model CK-40; Olympus Corporation) at x200 magnification.

Gelatin zymography for the detection of MMP-9. HepG2 cells were seeded into a six-well plate at density of 1x10⁶ per well and treated with the aforementioned concentrations of DHA and/or

DDP for 24 h at 37°C. Subsequently, 30 μl supernatant from each group was collected and resuspended in non-reducing Laemmli sample buffer and separated using SDS-PAGE on an 8% gel containing 1 mg/ml gelatin (Shanghai Yuanye Bio-technology, Co., Ltd.). Following electrophoresis, gels were washed using 2.5% Triton X-100 to remove any SDS before being incubated in substrate buffer (50 mM Tris buffer containing 5 mM CaCl₂; pH 8) for 18 h at 37°C. Gels were then stained with 0.5% Coomassie Brilliant Blue R-250 (Wuhan Servicebio Technology Co., Ltd.) for 3 h at room temperature, followed by de-staining for 2 h at room temperature. Gelatinolytic activity was visualized via imaging the negative staining bands using a digital camera. The acquired image results are analyzed by ImageJ 1.8.0. (National Institutes of Health).

Western blotting. HepG2 cells were treated with the aforementioned concentrations of DHA and/or DDP for 24 h at 37°C before being lysed on ice using RIPA lysis buffer (Beyotime Institute of Biotechnology) containing proteinase inhibitors. Protein samples in the lysate were quantified using a BCA kit (Beyotime Institute of Biotechnology) before being mixed with 5X loading buffer and 20 μg of protein in each lane was denatured for separation using SDS-PAGE on a 10% gel. The PVDF membrane onto which the protein was transferred was blocked with 5% skimmed milk at room temperature for 1 h. The membranes were incubated with primary antibodies against the following proteins at 4°C for 12 h: Fas (1:1,000; cat. no. K008079P; Beijing Solarbio Science & Technology

Co., Ltd.), Fas-associated death domain (FADD; 1:1,000; cat. no. K008372P; Beijing Solarbio Science & Technology Co., Ltd.), pro-caspase-3 (1:1,000; cat. no. sc-7272; Santa Cruz Biotechnology, Inc.), cleaved caspase-3 (1:1,000; cat. no. Asp175; Cell Signaling Technology, Inc.), pro-caspase-8 (1:1,000; cat. no. bsm33190M; Thermo Fisher Scientific, Inc.), cleaved caspase-8 (1:1,000; cat. no. Asp384; Cell Signaling Technology, Inc.), Bax (1:1,000; cat. no. K008076P; Beijing Solarbio Science & Technology Co., Ltd.), Bcl-2 (1:1,000; cat. no. K003505P; Beijing Solarbio Science & Technology Co., Ltd.), N-cadherin (1:1,000; cat. no. bs-1172R; BIOSS) and E-cadherin (1:1,000; cat. no. bs-1519R; BIOSS). The membranes were then washed by TBST (0.1% Tween-20) and incubated with goat anti-rabbit IgG secondary antibody (1:1,000; cat. no. SE134; Beijing Solarbio Science & Technology Co., Ltd.) and goat anti-mouse IgG secondary antibody (1:1,000; cat. no. bs-40296G-HRP; BIOSS) conjugated with HRP at room temperature for 2 h. β -actin was detected using anti- β -actin antibody (1:1,000; cat. no. K200058M; Beijing Solarbio Science & Technology Co., Ltd.) and was used as the loading control. Following incubation with the secondary antibody and ECL reagent (Wuhan Servicebio Biotechnology Co., Ltd.) the blots were imaged using a gel imaging system (ChemiDoc XRS+; Bio-Rad Laboratories, Inc.). The blots were semi-quantified using Image Lab™ software (version 5.0; MCM DESIGN).

Statistical analysis. SPSS 26.0 (IBM Corp.) software was used for data analysis. Data are presented as the mean \pm SD. One-way ANOVA followed by Tukey's post-hoc test was used for statistical comparisons among more than two groups. An unpaired Student's t-test were used for comparisons between two groups. $P < 0.05$ was considered to indicate a statistically significant difference.

Results

DHA enhances the effect of DDP on inhibiting HepG2 cell viability and proliferation. CCK-8 assay was used to detected the cell viability and the result showed that Both DHA and DDP exerted significant inhibitory effects on HepG2 cells compared with the untreated control group ($P < 0.05$; Fig. 1B and C). When the combination group was compared with the monotherapy group, there was no significant difference between the MD DDP group and the DHA + LD DDP group after treatment for 24 h ($P > 0.05$). The inhibition rate was significantly enhanced in the DHA + MD DDP group compared with the HD DDP group following treatment for 24 h ($P < 0.05$). After treatment for 48 h, the inhibition rate of both combination groups was significantly enhanced compared with the DDP-only groups ($P < 0.05$; DHA + LD DDP vs. MD DDP and DHA + MD DDP vs. HD DDP) (Fig. 1D). Furthermore, the number of colonies formed was significantly decreased in the combination groups compared with that of the DDP-only groups (Fig. 1E and F; $P < 0.05$; DHA + LD DDP vs. MD DDP and DHA + MD DDP vs. HD DDP). These data suggested that DHA may have enhanced the inhibitory effects of DDP on HepG2 cell proliferation.

DHA combined with DDP induces apoptosis and morphological changes in HepG2 cells. AO/EB dual-staining

was used to detect the apoptosis of HepG2 cells. Typically, green/yellow fluorescence is emitted in healthy cells stained with AO/EB, whereas apoptotic cells emit orange/red fluorescence. The results demonstrated that fluorescent green cells were the majority in the control group, with the number of cells fluorescing red or orange being markedly increased after treatment with DHA or DDP and increasing particularly in the combination groups treated with DHA and DDP (Fig. 2A). Furthermore, combined treatment significantly increased the apoptosis of HepG2 cells compared with the DDP-only groups ($P < 0.05$; DHA + LD DDP vs. MD DDP and DHA + MD DDP vs. HD DDP; Fig. 2B). As the percentage of apoptotic cells increased, the density of cells in the DHA and/or DDP treatment groups markedly decreased and the cell morphology became rounded and shrunken (data not shown).

Cell apoptosis was also detected using flow cytometry. Significantly increased apoptosis was detected in all treatment groups compared with the control group ($P < 0.05$). Compared with the DDP-only groups, the apoptotic rate was significantly increased in the combined groups ($P < 0.05$; DHA + LD DDP vs. MD DDP and DHA + MD DDP vs. HD DDP) (Fig. 2C and D). These results were consistent with the results of the dual AO/EB staining. In summary, DHA + LD DDP treatment resulted in apoptotic effects significantly greater than those observed with MD DDP, whereas DHA + MD DDP exerted a significantly greater apoptotic effect compared with HD DDP. These observations suggested that the extent of apoptosis in HepG2 cells induced by DDP could be enhanced by DHA.

DHA combined with DDP suppresses the migration of HepG2 cells. The migratory ability of HepG2 cells was detected using the wound healing and Transwell assays. Cells migrated to the center of the wound in the control group but this was significantly inhibited in the other treatment groups compared with the control ($P < 0.05$; Fig. 3A). Moreover, the migration rate of HepG2 cells in the combined treatment groups were significantly more inhibited compared with the DDP-only treatment groups ($P < 0.05$; DHA + LD DDP vs. MD DDP and DHA + MD DDP vs. HD DDP; Fig. 3B). Furthermore, the Transwell assay results demonstrated that a large number of cells in the control group migrated to the lower compartment, which demonstrated a potent migratory ability of HepG2 cells. However, the number of migratory cells decreased significantly when treated with DHA and/or DDP compared with the control. Combination treatment groups exhibited significantly greater reductions in migratory ability compared with the DDP-only treatment groups ($P < 0.05$; DHA + LD DDP vs. MD DDP and DHA + MD DDP vs. HD DDP) (Fig. 3C and D). Taken together, these data suggested that DHA combined with DDP may have inhibited the migration of HepG2 cells.

DHA in combination with DDP modulates the expression of apoptosis-related proteins. To determine if the expression levels of proteins associated with cell apoptosis were affected by DHA combined with DDP treatment in HepG2 cells, protein samples from HepG2 cells treated with DHA and/or DDP were semi-quantified using western blotting

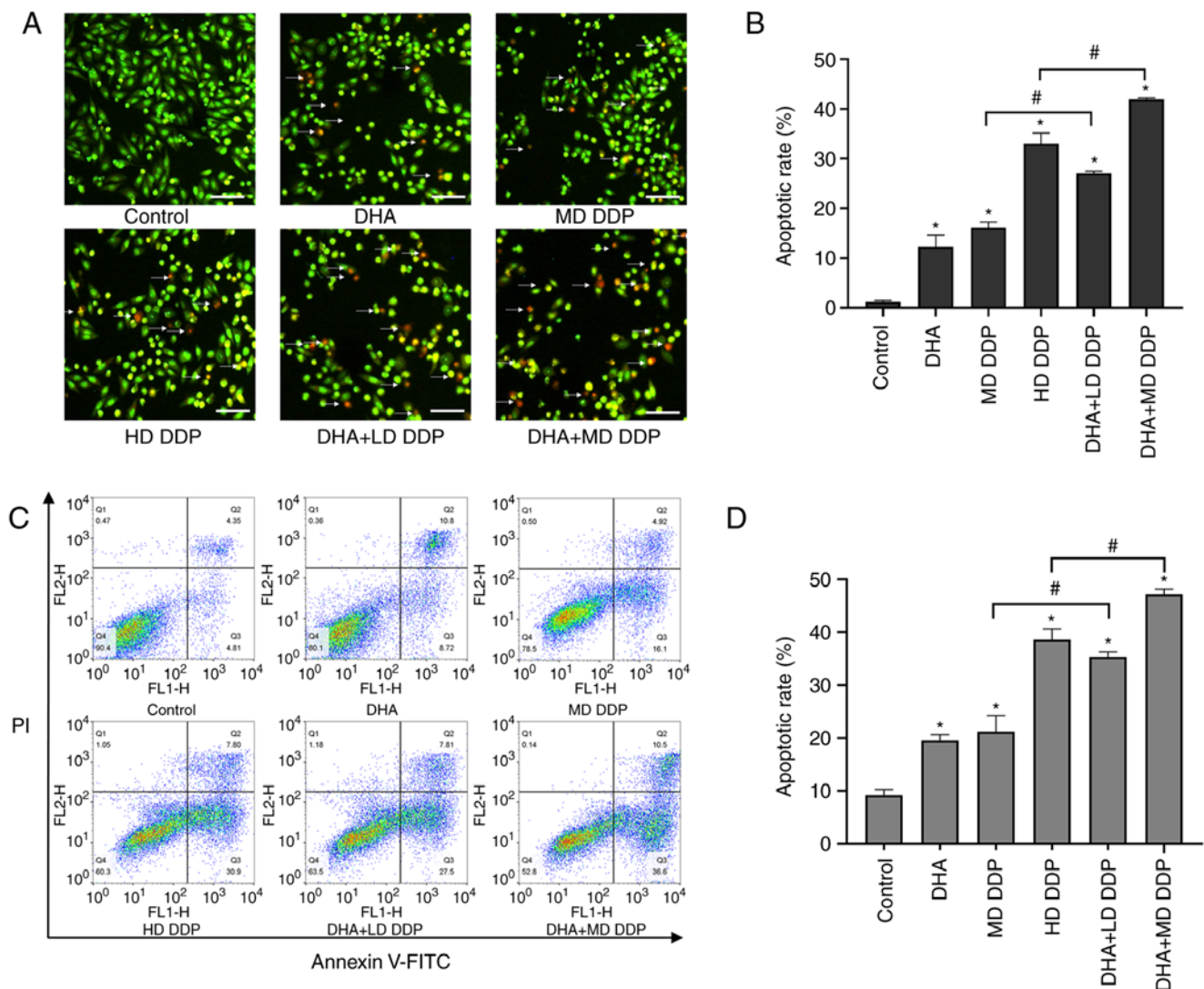


Figure 2. Apoptosis of HepG2 cells treated with DHA (100 μ M) and/or DDP. (A) Representative image of HepG2 cells treated with DHA and/or DDP for 24 h and dual-stained with AO/EB. Scale bar, 50 μ m, and arrows point to apoptotic cells. (magnification, x100). (B) Apoptotic rate of HepG2 cells was assessed using the AO/EB dual-staining assay. (C) Effect of DHA and/or DDP on the apoptosis of HepG2 cells was quantified via Annexin V-FITC/PI-staining flow cytometry. (D) Apoptotic rate of HepG2 cells assessed using the Annexin V-FITC/PI-staining flow cytometry assay. Data are presented as the mean \pm SD of more than three independent experiments. * P <0.05 vs. control; # P <0.05. DHA, dihydroartemisinin; DDP, cisplatin; AO, acridine orange; EB, ethidium bromide; LD, low dose (10 μ g/ml); MD, medium dose, (15 μ g/ml); HD, high dose, (20 μ g/ml).

(Fig. 4A-C). The relative protein expression levels were semi-quantified via gray value analysis (Fig. 4D). Significant increases in Fas FADD and Bax expression levels in DHA and/or DDP treatment groups were detected compared with that of the control group (P <0.05). Furthermore, this effect was significantly greater in the combination groups compared with the DDP-only groups (P <0.05; DHA + LD DDP vs. MD DDP and DHA + MD DDP vs. HD DDP). The ratio of cleaved caspase-3 to pro-caspase-3 and the ratio of cleaved caspase-8 to pro-caspase-8 were significantly increased in the DHA and DDP combination groups compared with the DDP-only groups (P <0.05). The relative protein expression levels of Bcl-2 were significantly decreased in the combination groups compared with the DDP-only groups. Overall, these data suggested that DHA potentially worked synergistically with DDP to enhance cell apoptosis via the modulation of Fas death receptor signaling pathway activity and the mitochondrial apoptosis signaling pathway in HepG2 cells.

DHA in combination with DDP regulates cadherin and MMP-9 expression. To further explore the mechanism underlying the effects of DHA combined with DDP on the migration of HepG2 cells, E-cadherin and N-cadherin protein expression levels were assessed in HepG2 cells using western blotting. Furthermore, the expression of MMP-9 in HepG2 cell culture supernatant was analyzed using gelatin zymography. The combined use of DHA and DDP significantly increased the protein expression levels of E-cadherin but significantly decreased the protein expression levels of N-cadherin compared with the untreated control and DDP-only groups (P <0.05; DHA + LD DDP vs. MD DDP and DHA + MD DDP vs. HD DDP; Fig. 5A). The expression of MMP-9 was significantly decreased when DHA was combined with DDP compared with the DDP-only groups (P <0.05; DHA + LD DDP vs. MD DDP and DHA + MD DDP vs. HD DDP) (Fig. 5E and F). In conclusion, DHA combined with DDP regulated expression of EMT-related protein and decreased the expression of MMP-9 in HepG2 cells.

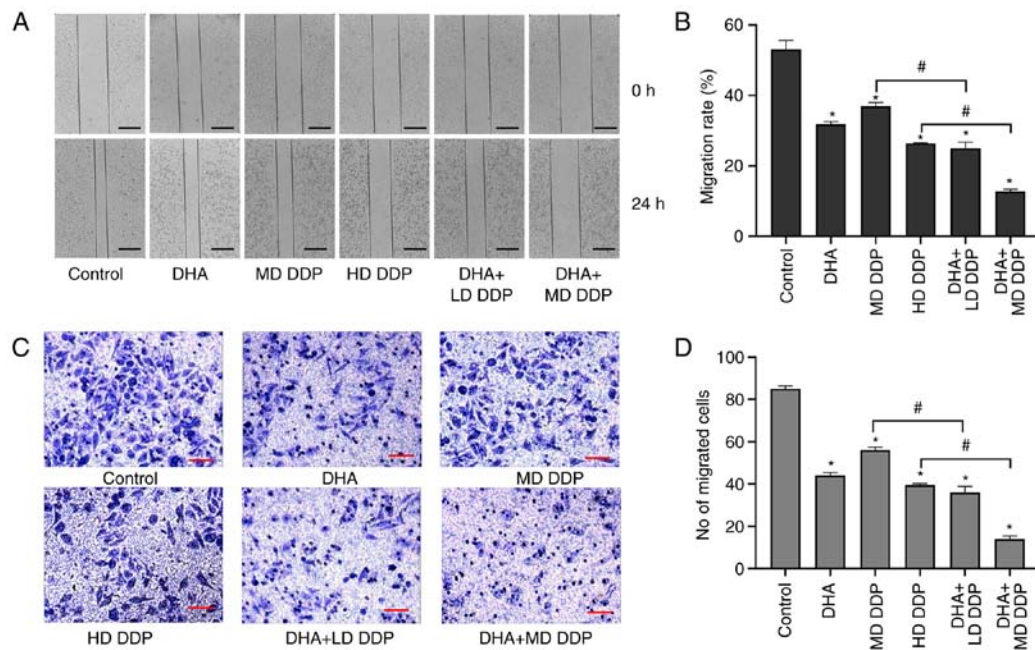


Figure 3. Migration abilities of HepG2 cells treated with DHA (100 μ M) and/or DDP were detected using the wound healing assay and Transwell assay. (A) Representative images of the wound healing assay at 0 and 24 h of HepG2 cells being treated with DHA and/or DDP. Scale bar, 2 mm. (B) Migration rate of HepG2 cells assessed using the wound healing assay. (C) Images of HepG2 cells that have migrated to the lower Transwell chamber following treatment with DHA and/or DDP. Scale bar is 25 μ m (magnification, x200). (D) Mean number of migrated cells in five fields of view per group. Data are presented as the mean \pm SD of more than three independent experiments. * P <0.05, vs. control; # P <0.05. DHA, dihydroartemisinin; DDP, cisplatin; LD, low dose (10 μ g/ml); MD, medium dose, (15 μ g/ml); HD, high dose, (20 μ g/ml).

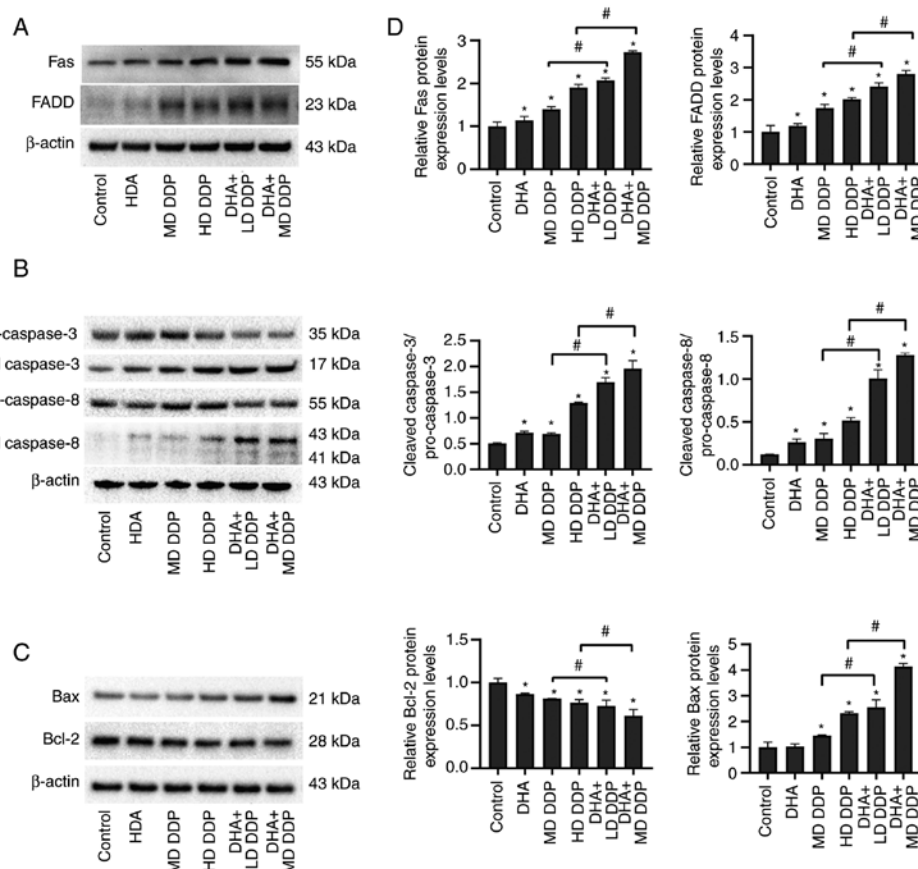


Figure 4. Apoptosis-associated proteins in HepG2 cells treated with DHA (100 μ M) and/or DDP were detected using western blotting. Effect of DHA and/or DDP on the protein expression levels of (A) Fas and FADD, (B) pro-caspase-3, cleaved caspase-3, pro-caspase-8 and cleaved caspase-8 and (C) Bax and Bcl-2 in HepG2 cells. β -actin was used as the loading control. (D) Relative protein expression levels of Fas, FADD, pro-caspase-3, cleaved caspase-3, pro-caspase-8, cleaved caspase-8, Bax and Bcl-2. Data are presented as the mean \pm SD of more than three independent experiments. * P <0.05 vs. control; # P <0.05. DHA, dihydroartemisinin; DDP, cisplatin; FADD, Fas-associated death domain; LD, low dose (10 μ g/ml); MD, medium dose, (15 μ g/ml); HD, high dose, (20 μ g/ml).

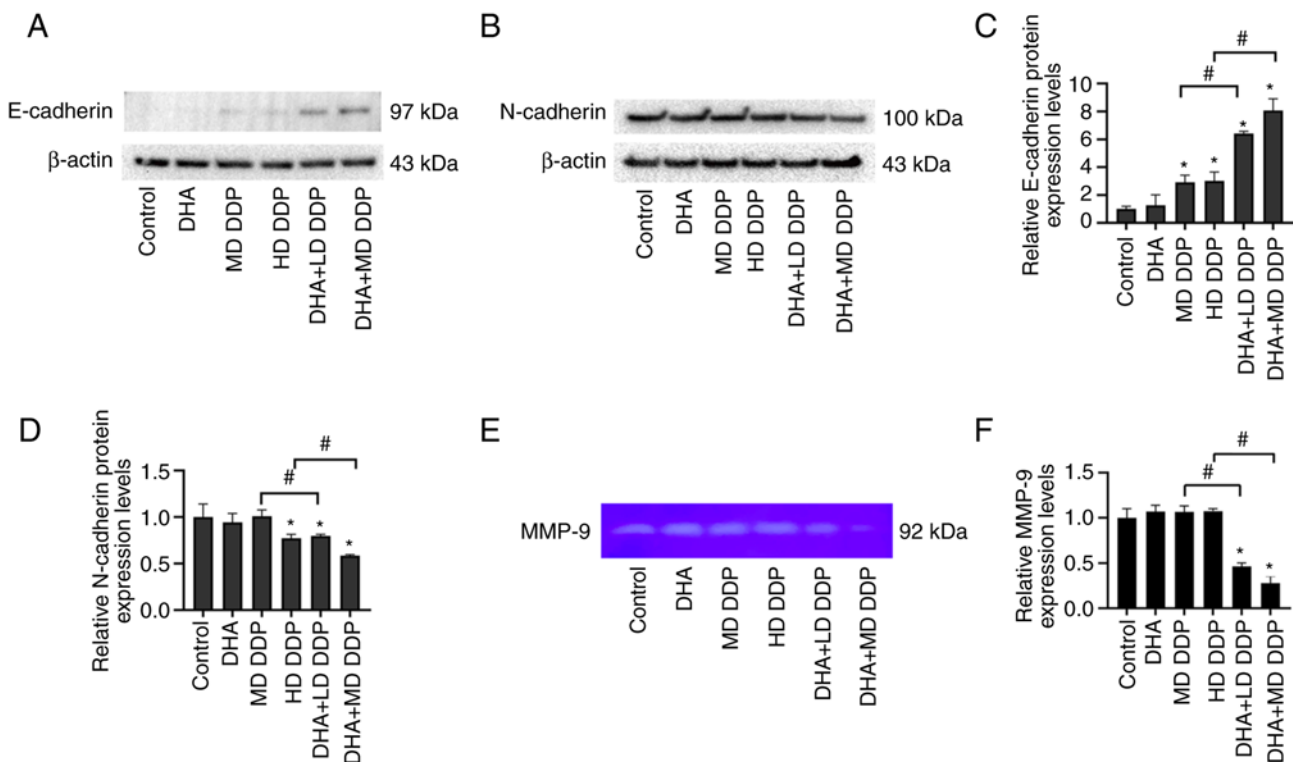


Figure 5. Cadherin and MMP-9 expression of HepG2 cells treated with DHA and/or DDP were detected via western blotting or gelatin zymography. (A and B) Effect of DHA and/or DDP on the protein expression levels of E-cadherin and N-cadherin in HepG2 cells. β -actin was used as an internal reference. (C and D) Relative protein expression levels of E-cadherin and N-cadherin. (E) Effect of DHA and/or DDP on the expression of MMP-9 in HepG2 cells. (F) Relative expression levels of MMP-9. Data are presented as mean \pm SD of more than three independent experiments. * $P < 0.05$ vs. control; # $P < 0.05$. DHA, dihydroartemisinin (100 μ M); DDP, cisplatin; LD, low dose (10 μ g/ml); MD, medium dose, (15 μ g/ml); HD, high dose, (20 μ g/ml).

Discussion

DDP-based chemotherapy serves an important role in the treatment of malignancies (21). However, drug resistance and adverse side effects have largely limited its application and efficacy (22). Therefore, the exploration of a novel DDP sensitizer agent would be of great therapeutic significance (23,24). Over the past decade, several naturally-occurring compounds have been reported to exert anti-tumor properties and can increase the efficacy of existing chemotherapeutic agents, while conferring minimal side effects and complications (25). A previous study reported that berberine, a compound extracted from Huang Lian and other Chinese medicinal herbs, displayed synergistic effects with DDP in inducing necroptosis and apoptosis of ovarian cancer cells. This was caused via the promotion of the expression of caspase-3, caspase-8, receptor interacting serine/threonine kinase 3 and mixed lineage kinase domain-like pseudokinase (24). Moreover, Abe *et al* (26) reported that caffeine citrate significantly improves the anti-cancer effects of DDP on osteosarcoma and fibrosarcoma cells via the inhibition of DNA repair induced by DDP. In the present study, DHA was demonstrated to enhance the anti-cancer effects of DDP, which provided additional evidence of the viability of DHA as a sensitizer of DDP for liver cancer therapy.

DHA is a naturally-occurring compound, that is primarily used for the treatment of malaria, and which exhibits superior bioavailability compared with artemisinin (27). Previous clinical and laboratory studies have demonstrated that DHA confers minimal adverse side effects (28,29). Furthermore,

a previous study reported that DHA exerts potent cytotoxic effects on liver cancer cells, including on the HepG2, Huh-7, BEL-7404 and Hep3B cell lines, but not on normal non-cancerous human liver cells (30). DHA has been previously explored as a potential sensitizer via synergy with other clinical anti-cancer agents, which enhanced their anti-cancer activity (31-33). Here, CCK-8 results revealed that both DHA and DDP alone inhibited HepG2 cell viability in a dose-dependent manner. However, the combination with DHA showed to achieve higher dose effects than even the lower dose of DDP, suggesting the possibility of reducing the dosage of chemotherapeutic agents by combination. Subsequent colony formation assays further validated the role of this combination in inhibiting HepG2 cell proliferation. Further study demonstrated that combining DHA and DDP significantly enhanced apoptosis and prevented cell migration in the HepG2 cell line, which supported the action of DHA as a viable DDP sensitizer in the aforementioned studies. These results provided primary experimental evidence for the therapeutic application of DHA in the treatment of liver cancer.

DNA damage and the activation of poly (ADP-ribose) polymerase to induce tumor cell apoptosis are important mechanisms underlying the anti-tumor effects of DDP (8). It has been previously reported that mitochondria and the Fas signaling pathway serve a key role in this type of apoptosis (34,35). However, suppression of apoptosis increases tumor cell drug resistance to DDP (9,36,37). According to previous studies, the Fas receptor signaling pathway and the mitochondrial apoptosis signaling pathway are both closely

associated with DHA-induced tumor cell apoptosis (38,39). In the present study, apoptosis of HepG2 cells treated with DHA and/or DDP and the protein expression levels of Fas, FADD, pro-caspase-3, cleaved caspase-3, pro-caspase-8, cleaved caspase-8, Bax and Bcl-2 were all assessed. This suggested that the Fas receptor signaling pathway and the mitochondrial apoptosis signaling pathway potentially serve a vital role in DHA/DDP-induced apoptosis in liver cancer cells.

The epithelial-mesenchymal transition (EMT) is mainly associated with the migration and invasion of tumor cells and is one of the main factors of tumor progression (40). Numerous studies have previously demonstrated that the EMT serves a key contributing role in chemoresistance (41,42). Furthermore, E-cadherin and N-cadherin are known markers of the EMT, whereas MMP-9 can degrade the extracellular matrix following the EMT (43). In the present study, the migratory ability of liver cancer cells was significantly inhibited by DHA combined with DDP. In studying the potential molecular mechanisms of cell metastasis, enzyme profiling and protein blotting showed that DDP combined with DHA treatment downregulated the expression levels of N-calmodulin and MMP-9, as well as up-regulated expression of E-calmodulin in HepG2 cells. Based on this, we hypothesized that DDP can inhibit EMT in HepG2 cells in combination with DHA, and is the mechanism by which DHA improves DDP drug resistance.

In conclusion, DHA significantly enhanced the effects of DDP on the proliferation, apoptosis and migration of HepG2 cells. These results suggested that DHA has the potential for application as a novel anti-tumor sensitizer of DDP and provided an experimental basis for the use of DHA as a clinical anti-tumor drug in combination with DDP. Further studies are required to assess DNA damage and the effect on the cell cycle in liver cancer cells of this combined treatment. Furthermore, *in vivo* study of this combination therapy will also be necessary in subsequent studies.

Acknowledgements

Not applicable.

Funding

The present study was supported by the Chinese Academy of Medical Sciences Innovation Fund for Medical Sciences (grant no. 2018-I2M-AI-015) and the National Science Foundation of China (grant no. 81702920).

Availability of data and materials

The datasets used and/or analyzed during the current study are available from the corresponding author on reasonable request.

Authors' contributions

QR performed the experiments, analyzed the data and drafted the manuscript. RL performed the western blotting experiments. HY, LX and BH performed the cell culture assay and analyzed the data. GZ and FW designed the study, conceived the experiments, laid out the experimental scheme, confirm the authenticity of all the raw data, and revised the manuscript.

All the authors read and approved the final version of the manuscript to be published.

Ethics approval and consent to participate

Not applicable.

Patient consent for publication

Not applicable.

Competing interests

The authors declare that they have no competing interests.

References

1. Sung H, Ferlay J, Siegel RL, Laversanne M, Soerjomataram I, Jemal A and Bray F: Global cancer statistics 2020: GLOBOCAN estimates of incidence and mortality worldwide for 36 cancers in 185 countries. *CA Cancer J Clin* 71: 209-249, 2021.
2. Wang Y, Liu Y, Liu Y, Zhou W, Wang H, Wan G, Sun D, Zhang N and Wang Y: A polymeric prodrug of cisplatin based on pullulan for the targeted therapy against hepatocellular carcinoma. *Int J Pharm* 483: 89-100, 2015.
3. El Dika I, Makki I and Abou-Alfa GK: Hepatocellular carcinoma, novel therapies on the horizon. *Chin Clin Oncol* 10: 12, 2021.
4. Anwanwan D, Singh SK, Singh S, Saikam V and Singh R: Challenges in liver cancer and possible treatment approaches. *Biochim Biophys Acta Rev Cancer* 1873: 188314, 2020.
5. Gurzu S, Kobori L, Fodor D and Jung I: Epithelial mesenchymal and endothelial mesenchymal transitions in hepatocellular carcinoma: A review. *Biomed Res Int* 2019: 2962580, 2019.
6. Demir T, Lee SS and Kaseb AO: Systemic therapy of liver cancer. *Adv Cancer Res* 149: 257-294, 2021.
7. Dutta S, Mahalanobish S, Saha S, Ghosh S and Sil PC: Natural products: An upcoming therapeutic approach to cancer. *Food Chem Toxicol* 128: 240-255, 2019.
8. Ghosh S: Cisplatin: The first metal based anticancer drug. *Bioorg Chem* 88: 102925, 2019.
9. Fuertes MA, Alonso C and Pérez JM: Biochemical modulation of cisplatin mechanisms of action: Enhancement of antitumor activity and circumvention of drug resistance. *Chem Rev* 103: 645-662, 2003.
10. Oun R and Rowan E: Cisplatin induced arrhythmia; electrolyte imbalance or disturbance of the SA node? *Eur J Pharmacol* 811: 125-128, 2017.
11. Pabla N and Dong Z: Cisplatin nephrotoxicity: Mechanisms and renoprotective strategies. *Kidney Int* 73: 994-1007, 2008.
12. Santos NAGD, Ferreira RS and Santos ACD: Overview of cisplatin-induced neurotoxicity and ototoxicity, and the protective agents. *Food Chem Toxicol* 136: 111079, 2020.
13. Astolfi L, Ghiselli S, Guaran V, Chicca M, Simoni E, Olivetto E, Lelli G and Martini A: Correlation of adverse effects of cisplatin administration in patients affected by solid tumours: A retrospective evaluation. *Oncol Rep* 29: 1285-1292, 2013.
14. Miller LH and Su X: Artemisinin: Discovery from the Chinese herbal garden. *Cell* 146: 855-858, 2011.
15. Ma N, Zhang Z, Liao F, Jiang T and Tu Y: The birth of artemisinin. *Pharmacol Ther* 216: 107658, 2020.
16. Haynes RK: From artemisinin to new artemisinin antimalarials: Biosynthesis, extraction, old and new derivatives, stereochemistry and medicinal chemistry requirements. *Curr Top Med Chem* 6: 509-537, 2006.
17. Dai X, Zhang X, Chen W, Chen Y, Zhang Q, Mo S and Lu J: Dihydroartemisinin: A potential natural anticancer drug. *Int J Biol Sci* 17: 603-622, 2021.
18. Chen X, He LY, Lai S and He Y: Dihydroartemisinin inhibits the migration of esophageal cancer cells by inducing autophagy. *Oncol Lett* 20: 94, 2020.
19. Wu L, Pang Y, Qin G, Xi G, Wu S, Wang X and Chen T: Farnesylthiosalicylic acid sensitizes hepatocarcinoma cells to artemisinin derivatives. *PLoS One* 12: e0171840, 2017.

20. Zhang R, Niu Y and Zhou Y: Increase the cisplatin cytotoxicity and cisplatin-induced DNA damage in HepG2 cells by XRCC1 abrogation related mechanisms. *Toxicol Lett* 192: 108-114, 2010.
21. Raudenska M, Balvan J, Fojtů M, Gumulec J and Masarik M: Unexpected therapeutic effects of cisplatin. *Metallomics* 11: 1182-1199, 2019.
22. Kiss RC, Xia F and Acklin S: Targeting DNA damage response and repair to enhance therapeutic index in cisplatin-based cancer treatment. *Int J Mol Sci* 22: 8199, 2021.
23. Sun Y, Jiang W, Lu W, Song M, Liu K, Chen P, Chang A, Ling J, Chiao PJ, Hu Y and Huang P: Identification of cisplatin sensitizers through high-throughput combinatorial screening. *Int J Oncol* 53: 1237-1246, 2018.
24. Liu L, Fan J, Ai G, Liu J, Luo N, Li C and Cheng Z: Berberine in combination with cisplatin induces necroptosis and apoptosis in ovarian cancer cells. *Biol Res* 52: 37, 2019.
25. Rejchová A, Opattová A, Čumová A, Slíva D and Vodička P: Natural compounds and combination therapy in colorectal cancer treatment. *Eur J Med Chem* 144: 582-594, 2018.
26. Abe K, Yamamoto N, Hayashi K, Takeuchi A and Tsuchiya H: Caffeine citrate enhanced cisplatin antitumor effects in osteosarcoma and fibrosarcoma in vitro and in vivo. *BMC Cancer* 19: 689, 2019.
27. Tu Y: The discovery of artemisinin (qinghaosu) and gifts from Chinese medicine. *Nat Med* 17: 1217-1220, 2011.
28. Angus B: Novel anti-malarial combinations and their toxicity. *Expert Rev Clin Pharmacol* 7: 299-316, 2014.
29. Wan X, Zhong H, Pan W, Li Y, Chen Y, Li N and Tang B: Programmed release of dihydroartemisinin for synergistic cancer therapy using a CaCO₃ mineralized metal-organic framework. *Angew Chem Int Ed Engl* 58: 14134-14139, 2019.
30. Im E, Yeo C, Lee HJ and Lee EO: Dihydroartemisinin induced caspase-dependent apoptosis through inhibiting the specificity protein 1 pathway in hepatocellular carcinoma SK-Hep-1 cells. *Life Sci* 192: 286-292, 2018.
31. Li Q, Ma Q, Cheng J, Zhou X, Pu W, Zhong X and Guo X: Dihydroartemisinin as a sensitizing agent in cancer therapies. *Onco Targets Ther* 14: 2563-2573, 2021.
32. Tai X, Cai XB, Zhang Z and Wei R: In vitro and in vivo inhibition of tumor cell viability by combined dihydroartemisinin and doxorubicin treatment, and the underlying mechanism. *Oncol Lett* 12: 3701-3706, 2016.
33. Jin H, Jiang AY, Wang H, Cao Y, Wu Y and Jiang XF: Dihydroartemisinin and gefitinib synergistically inhibit NSCLC cell growth and promote apoptosis via the Akt/mTOR/STAT3 pathway. *Mol Med Rep* 16: 3475-3481, 2017.
34. Dasari S, Njiki S, Mbemi A, Yedjou CG and Tchounwou PB: Pharmacological effects of cisplatin combination with natural products in cancer chemotherapy. *Int J Mol Sci* 23: 1532, 2022.
35. Qi L, Luo Q, Zhang Y, Jia F, Zhao Y and Wang F: Advances in toxicological research of the anticancer drug cisplatin. *Chem Res Toxicol* 32: 1469-1486, 2019.
36. Makovec T: Cisplatin and beyond: Molecular mechanisms of action and drug resistance development in cancer chemotherapy. *Radiol Oncol* 53: 148-158, 2019.
37. Zhou J, Kang Y, Chen L, Wang H, Liu J, Zeng S and Yu L: The drug-resistance mechanisms of five platinum-based antitumor agents. *Front Pharmacol* 11: 343, 2020.
38. Mao H, Gu H, Qu X, Sun J, Song B, Gao W, Liu J and Shao Q: Involvement of the mitochondrial pathway and Bim/Bcl-2 balance in dihydroartemisinin-induced apoptosis in human breast cancer in vitro. *Int J Mol Med* 31: 213-218, 2013.
39. Hu YJ, Zhang JY, Luo Q, Xu JR, Yan Y, Mu LM, Bai J and Lu WL: Nanostructured dihydroartemisinin plus epirubicin liposomes enhance treatment efficacy of breast cancer by inducing autophagy and apoptosis. *Nanomaterials (Basel)* 8: 804, 2018.
40. Wang Y, Liu Y, Xiang L, Han L, Yao X, Hu Y and Wu F: Cyclin D1b induces changes in the macrophage phenotype resulting in promotion of tumor metastasis. *Exp Biol Med (Maywood)* 246: 2559-2569, 2021.
41. Bao Y, Zhang Y, Lu Y, Guo H, Dong Z, Chen Q, Zhang X, Shen W, Chen W and Wang X: Overexpression of microRNA-9 enhances cisplatin sensitivity in hepatocellular carcinoma by regulating EIF5A2-mediated epithelial-mesenchymal transition. *Int J Biol Sci* 16: 827-837, 2020.
42. Du B and Shim JS: Targeting epithelial-mesenchymal transition (EMT) to overcome drug resistance in cancer. *Molecules* 21: 965, 2016.
43. Pastushenko I and Blanpain C: EMT transition states during tumor progression and metastasis. *Trends Cell Biol* 29: 212-226, 2019.



This work is licensed under a Creative Commons Attribution-NonCommercial-NoDerivatives 4.0 International (CC BY-NC-ND 4.0) License.